Hemispheric Spectral Statistics of Available Potential Energy

FERDINAND BAER

Dept. of Atmospheric and Oceanic Science, The University of Michigan, Ann Arbor 48104

(Manuscript received 17 May 1973, in revised form 27 January 1974)

ABSTRACT

Analysis of hemispheric temperature variance data on five isobaric surfaces in terms of two-dimensional spectral decomposition shows that the available potential energy distributes with a slope in the neighborhood of -3 for the scale range $14 \leqslant n \leqslant 25$. Although this slope varies with pressure, indications are that the observations substantiate the expectations of geostrophic turbulence theory. The noted deviations from -3 are discussed in terms of the distribution of energy in vertical modes which are not in the range in which -3 statistics should be expected. Vertical scales necessary for a three-dimensional spectral representation are considered with regard to the Brunt-Väisälä frequency distribution.

1. Introduction

Although atmospheric predictability may be limited theoretically, as suggested by Lorenz (1969), the accuracy of weather prediction in time is closely related to how well one parameterizes that part of the flow which is outside the predictable scale range. The fact that simple truncation—either finite-difference or spectral—has not been adequate for prediction accuracy has led to studies in search of statistical properties of subgrid-scale phenomena which, if time invariant, could be used parametrically in models. The first statistics to be considered were based on Kolomogoroff's theory of the inertial subrange, indicating an energy decay with wavenumber to a $-5/3$ power, but the applicable scales were so small that the results were useless to planetary- and synoptic-scale forecasting.

Subsequent theoretical and computational developments by Kraichnan (1967), Leith (1971) and Lilly (1969) indicated that the statistics of kinetic energy decay with wavenumber were given by a -3 power law. These results were applicable in a scale range commensurate with those scales actually predicted in forecasting models; however, they were derived for two-dimensional flow whereas the prediction models are applicable to a three-dimensional fluid. Thus, one requires statistics on available potential energy as well as kinetic energy.

Noting these limitations, Charney (1971) extended the two-dimensional turbulence theory to three dimensions using the concept of geostrophic turbulence and represented by the potential vorticity equation. By applying a number of approximations, Charney was able to show that not only kinetic energy but also available potential energy should decay in the wave domain by a -3 power law. Should the conditions postulated by Charney apply in the prediction range of atmospheric models, a basis for parameterizing subgrid-scale temperature as well as momentum correlations has been established.

Since available potential energy is proportional to temperature variance in geostrophic flow, an ideal test of Charney's developments could be performed by an analysis of temperature data in a three-dimensional wavenumber representation. Unfortunately, this has not yet been done. Indeed, Charney was able to test his expectations against data represented only in a one-dimensional spectra. Although the condition of isotropy imposed by Charney should make this adequate, a one-dimensional spectra on a given latitude circle is not generally isotropic with a two-dimensional spectra.

We may see this from an expansion of temperature in a two-dimensional surface in terms of solid harmonics [see Eq. (11)] wherein the expansion coefficients are denoted as $T_{n,l}$. The temperature variance in the surface, representative of the available potential energy and expressed by (12), involves an integration over the two-dimensional surface. Completion of this integration allows the representation to be stated in terms of scale-dependent amplitudes. The sums over the two scale indices l and n may be interchanged such that

$$P=\sum_{n=0}^{\infty}\sum_{l=-n}^{n}|T_{n,l}|^2=\sum_{l=0}^{\infty}\sum_{n=l}^{\infty}(2-\delta_{l,0})|T_{n,l}|^2,$$

$$=\sum_{n=0}^{\infty}P_2(n)=\sum_{l=0}^{\infty}P_1(l),$$

where

$$P_2(n)=\sum_{l=0}^{n}(2-\delta_{l,0})|T_{n,l}|^2,$$

$$P_1(l)=\sum_{n=l}^{\infty}(2-\delta_{l,0})|T_{n,l}|^2.$$

If we now invoke the condition of isotropy and note that n is a characteristic scale number in two dimensions, we state that $|T_{n,l}| = T(n)$ only, we find that $P_2 = (2n+1)|T_{n,l}|^2$, and thus,

$$P_1(l) = \sum_{n=l}^{\infty} \frac{2-\delta_{l,0}}{2n+1} P_2(n).$$

The implication of the isotropy assumption is that it holds for all scales, yet the model described by Charney is scale-dependent in its development. If, however, the amplitude of energy is negligible in the smaller scales, we may find the expected statistics in observations. We shall subsequently test the relevance of the isotropy assumption in our data samples by comparing $P_1(l)$ as it depends on $P_2(n)$ with its dependence on $T_{n,l}$.

Reference to Eq. (12) indicates that an expression for energy structure in the scale-dependent domain requires an integration over the entire space domain. It can easily be shown that integration over only one dimension (say longitude) will generate a spectral distribution which is latitude-dependent, thus allowing distributions which vary from one latitude to another. In comparing the one- and two-dimensional spectra under the isotropic assumption, therefore, we must carry out the integration over the entire spatial surface. Nevertheless, the spectral characteristics to be found from atmospheric observations are substantially more limited in the short-wave scale for the one-dimensional representation (Baer, 1972; Julian *et al.*, 1970) and thus we may expect a better comparison to theory from the two-dimensional spectra.

Unfortunately, the theory as proposed by Charney requires isotropy in three dimensions (provided the vertical dimension is properly scaled). Several three-dimensional spectral representations have been proposed, but to this writer's knowledge, no hemispheric data have been analyzed in that manner. Yet to assure the existence of spectral statistics in observational data which correspond to theoretical expectations, proper spectral ranges of data must be chosen. It should be evident to the reader that the limitations imposed on analysis of one-dimensional data based on two-dimensional isotropy are also applicable to two-dimensional analyses based on three-dimensional isotropy; i.e., if the analyses are made in pressure surfaces they should be vertically integrated so that the three-dimensional statistics will appear in the two-dimensional analyses.

On the assumption that the atmospheric static stability may be characterized by a simple pressure-dependent function, the potential vorticity equation will yield eigenfunctions in all three dimensions and the vertical scales will then be defined by the appropriate vertical eigenvalues. Based on such a model of the potential vorticity equation, we shall attempt to indicate the vertical scale range for which three-dimensional analyses of the spectral functions of energy may be calculated.

Since hemispheric analyses of temperature data (as representative of available potential energy) are limited in vertical resolution, we have made two-dimensional spectral distributions of available potential energy on several isobaric surfaces and compared these spectral statistics to those for one-dimensional representations, noting, of course, the limitations of no vertical integration when comparing the results to theoretical expectations. Such spectra for kinetic energy have already been presented by the writer (Baer, 1972). The two-dimensional representation is made in terms of associated Legendre polynomials and characterized by a scale index which is the order of these polynomials. The appropriateness of this two-dimensional index has been discussed by Baer (1972). The eigensolutions of the potential vorticity equation in the vertical coordinate should indicate how valid the two-dimensional spectral statistics are for comparison with and justification of the three-dimensional theory.

2. Three-dimensional scaling

To validate the existence of spectral statistics for both kinetic and available potential energy in atmospheric data as suggested by quasi-geostrophic theory, we must first find an appropriate scale representation in which to expand the data. Since the three-dimensional geostrophic theory as presented by Charney (1971) involves the solution of the potential vorticity equation, the appropriate scale functions (eigenfunctions) and their corresponding wavenumbers (eigenvalues) should be characteristic solutions to the equation for potential vorticity. On this basis Charney was able to predict a -3 decay of energy for both kinetic and potential energy, a decay applicable in any or all dimensions because of isotropy.

Since the appropriate equation which advances the statistical theory involves conservation of relative potential vorticity, the advection of earth's vorticity is considered negligible. The validity of this assumption will be considered subsequently. Accepting this assumption for the following development, we find that pertinent three-dimensional scaling will result from selecting the eigenfunctions $\psi_{n,i}$ of the potential vorticity equation such that

$$L\psi_{n,i} = -\gamma_{n,i}^2 \psi_{n,i}, \tag{1}$$

where the operator L has been defined by Charney as

$$L = \nabla^2 + \frac{f_0^2}{\bar{\rho}} \frac{\partial}{\partial z}\left(\frac{\bar{\rho}}{N^2}\frac{\partial}{\partial z}\right), \tag{2}$$

and the constants $\gamma_{n,i}^2$ representing the eigenvalues can be considered as wave (scale) numbers. The Laplacian (∇^2) is taken over two dimensions in a horizontal surface which we shall consider a spherical surface representing geopotential surfaces over the earth. The other symbols are standard: f_0 represents a mean Coriolis

TABLE 1. Lapse rates (°K km^{-1}) for selected indices m.

m	γ
3	8.54
4	6.12
6	4.88

parameter, $\bar{\rho}$ a standard density varying in the vertical (z) direction, and N^2 the Brunt-Väisälä frequency

$$N^2=\frac{g}{T}(\gamma_d-\gamma), \tag{3}$$

where γ_d is the dry adiabatic lapse rate and γ the observed lapse rate. Since the operators in the horizontal surface and in height are additive, the scale function ($\psi_{n,i}$) may be represented as the product of a horizontal times a vertical function, i.e.,

$$\psi_{n,i}=Y_n^l(\lambda,\mu)\cdot G_i(z), \tag{4}$$

where λ and μ represent longitude and sine of latitude respectively.

It has been shown by Baer (1972) that the appropriate scaling functions in the horizontal spherical surface are the associated Legendre functions which satisfy the equation

$$\nabla^2 Y_n^l(\lambda,\mu)=-n\frac{(n+1)}{a^2}Y_n^l(\lambda,\mu), \tag{5}$$

where n is the order of the Legendre function (also closely proportional to the scale number in two dimensions) and a is the mean radius of the earth.

The vertical scale can be set only when the distributions of N^2 and $\bar{\rho}$ are established. Charney simplified this representation by letting $\bar{\rho}\approx\rho_0 e^{-z/H}$, where H is the scale height of the atmosphere, and assuming that the scale of variation in N^2 is large compared to the vertical scale of turbulence. The assumption on $\bar{\rho}$ is reasonable (although not essential) whereas the assumption on N^2 may be questioned, especially near the tropopause. We shall select the vertical scales from the equation

$$\frac{f_0}{\bar{\rho}}\frac{\partial}{\partial z}\left(\frac{\bar{\rho}}{N^2}\frac{\partial G_i}{\partial z}\right)=f_0^2\frac{d}{d\zeta}q(\zeta)\frac{dG_i}{d\zeta}=-\gamma_i^2 G_i(\zeta), \tag{6}$$

with the distribution of N^2 based on observational information. Two separate studies have been performed in which solutions have been given to (6), both in terms of Bessel functions and both involving a statement of the stability function N^2.

The first solution, in which N^2 was calculated based on a constant-lapse atmosphere, was given by Wiin-Nielsen (1971). Although this approximation violates our observations of the upper atmosphere, a numerical study of a constant-lapse atmosphere with an isothermal layer on top was performed by McFarlane (1971) with the result that the eigenvalues (scales) of this layered model were not significantly changed from those derived from the constant-lapse atmosphere. In consequence, the solutions of Wiin-Nielsen take on added credibility. The constant-lapse condition makes the Brunt-Väisälä frequency inversely proportional to the temperature [Eq. (3)] and use of the ideal gas law and the hydrostatic approximation leads to the functional form of $q(\zeta)$

$$\left.\begin{aligned} q(\zeta)&=\frac{\zeta^2-\kappa\Gamma}{\kappa(1-\kappa)c^2(1-\Gamma)}\\ \zeta&\equiv\frac{P}{P_0}\approx e^{-z/H}\end{aligned}\right\}, \tag{7}$$

where $\kappa\equiv R/c_p$, $c^2=\hat{\gamma}RT_0$ (the Newtonian sound speed), and $\Gamma\equiv\gamma/\gamma_d$, the ratio of the lapse rate to dry adiabatic lapse rate. Since we do not choose unstable lapse conditions, $\Gamma\leqslant 1$, and we follow Wiin-Nielsen in defining $\kappa\Gamma=1/(m+1)$, $m>2.48$ for dry air. Values of $m=3$, 4 and 6 refer to lapse rates as listed in Table 1.

Substitution of m for $\kappa\Gamma$ in (7) leads to solutions for G_i in terms of Bessel functions of order m:

$$G_i=\zeta^{m/[-2(m+1)]}J_m(\lambda_i\zeta^{1/[2(m+1)]}), \tag{8}$$

where the roots have been chosen to satisfy the no flux condition at $\zeta=0$ and no vertical velocity at the bottom, $\zeta=1$. The values of the first ten roots (eigenvalues) for $m=3$, 4, 6 have been listed in Table 2, scaled to correspond to $[n(n+1)]^{\frac{1}{2}}$.

An alternate solution to (6) was presented by Simons (1968). Instead of a constant lapse rate, he assumed that the inverse static stability was given as a linear function of the pressure, such that

$$q(\zeta)=a+b\zeta.$$

The basis for this assumption derives from data, and Simons calculated the coefficients a and b from the stability data of Gates (1961) with surprising fidelity. The lapse rate resulting from this model atmosphere is

$$\gamma=\gamma_d-\frac{gp^2}{R^2T}(a+b\zeta)^{-1},$$

and the temperature distribution may be established by integration. Above the tropopause a very thin, stable inactive layer is superimposed, the whole configuration yielding solutions to (6) in terms of Bessel functions of zero order ($m=0$). The first ten roots of Simons solution are also listed in Table 2. Comparison of the roots in Table 2 suggests that Simons' model is somewhat less stable than Wiin-Nielsen's.

The scale range in which the expected statistics (−3 slope) should prevail must satisfy the approximations applicable to the theoretical development. On the long-wave end, the scales should be shorter than the primary

TABLE 2. First ten roots of Bessel function of order m scaled to correspond to $[n(n+1)]^{\frac{1}{2}}$.

Order m	Root i 1	2	3	4	5	6	7	9	8	10
0	14.1	25.7	37.3	48.9	60.4	72.	83.5	95.	106.6	118.1
3	9.7	14.2	18.5	22.6	26.6	30.9	34.9	39.	43.1	47.1
4	6.1	8.6	10.9	13.2	15.5	17.7	19.9	22.1	24.4	26.6
6	4.4	5.9	7.3	8.6	9.9	11.2	12.5	13.7	15.	16.3

baroclinically active scales, whereas the short-wave end must still satisfy the geostrophic approximation, while throughout the range the advection of relative vorticity must dominate advection of the earth's vorticity. Analysis of two-dimensional kinetic energy spectra in terms of the index $[n(n+1)]^{\frac{1}{2}}$ indicates that $n\approx 14$ was a reasonable lower scale index and $n\approx 25$ was the upper limit (Baer, 1972). The upper scale index was established in terms of the limitation in data content rather than on physical reasoning, but since the assessment of the theory must be made from observations, we shall use this value. If the advection of the earths' vorticity is to remain small relative to advection of relative vorticity, the kinetic energy in the wave components must decay less rapidly than n^{-4}, where n is the characteristic scale number (either one- or two-dimensional). The data presented by Baer (1972) indicate that this is so for the two-dimensional representation, but the slope of the one-dimensional representation is steeper than -4. For wavenumber 15, the wave velocity amplitude should exceed about 2.5 m sec^{-1} for relative advection to dominate. Characteristic velocities taken from Baer (1972) indicate that the velocity in the two-dimensional wave ($n=15$) is 3–3.5 m sec^{-1}, and, since the spectrum decays with a slope less than -4, the advection of relative vorticity predominates. The characteristic velocity of scale $l=15$ (one-dimensional) based on data taken from the source referenced above is 1.4–1.7 m sec^{-1} (which is less than 2.5 m sec^{-1}) and furthermore the spectral decay has a slope steeper than -4. Thus, the one-dimensional data will prove inadequate to test the turbulence theory of Charney. This latter conclusion is undoubtedly due to the lack of reliability in the one-dimensional data for scales in excess of wavenumber 18.

Returning now to three-dimensional considerations, but accepting the scale range to be given by two-dimensional reasoning because of data limitations, we shall direct our attention to the scale range 14–25 as appropriate wavenumbers in which the -3 statistics might exist. Note that we should expect to find the statistics in both the kinetic and available potential energy as suggested by Charney's development. A view of Table 2 shows clearly that not all the vertical modes fall into the desired scale range. It is generally observed that most of the variance in the vertical of atmospheric energy is in the lowest modes—hence the use of two- and three-level models. Except for the model proposed by Simons, we see from Table 2 that the first few modes in the vertical (roots 1 and 2) have larger characteristic scales than those in which we expect to find statistical turbulence. It is not sufficient, however, to assume that the vertical amplitude distribution of each horizontal scale compares to the observations alluded to above, since those observations apply to the largest planetary scales whereas we are interested in shorter (nonbaroclinically forced) scales. Such amplitude distributions are currently not available, principally because detailed vertical data on a hemispheric scale have not been readily accessible. Thus, it is conceivable, for the range of scales here considered (14–25), that most of the variance in the vertical exists in modes which are in this scale range. If most of the amplitude in the vertical is in scales outside this range, say scales $i=1, 2, 3$ for $m=4$ in Table 2, then the statistical expectations must be sought from the distribution of energy in the modes ($i>3$) which are in the 14–25 scale number range. Should the amplitudes of the lowest modes be negligible, then the entire vertical representation could be used to test for a statistical distribution; such a representation could then be found by analyzing the energy in a pressure surface, since all modes are involved in any pressure surface.

Observations of the spectral distribution of available potential energy in a pressure surface in terms of the two-dimensional index should give some indication of the amplitude distribution in the vertical modes. If the distribution is near -3 one may anticipate that the amplitude is predominantly in scales 14–25. Alternately, if the distribution approaches -5, we may suspect that the principal amplitude is in the lowest vertical modes. This result, first expressed by Merilees and Warn (1972), may be seen as follows. From (1), (4), (5) and (6) we note that the energy in any three-dimensional scale is represented as

$$E(\gamma_{n,i})=A(\gamma_{n,i})+K(\gamma_{n,i})=\gamma_{n,i}^2|\psi_{n,i}|^2, \propto \gamma_{n,i}^{-3}, \quad (9)$$

where E represents the total energy, A and K the available potential and kinetic energy, respectively, and ψ the streamfunction. The scale index is composed of the vertical index γ_i and the two-dimensional index $[n(n+1)]^{\frac{1}{2}}$ in the form, $\gamma_{n,i}^2=\gamma_i^2+n(n+1)$ and allows the energies to be expressed as

$$A(\gamma_{n,i})=\gamma_i^2|\psi_{n,i}|^2;\ K(\gamma_{n,i})=n(n+1)|\psi_{n,i}|^2. \quad (10)$$

If we now consider the first mode (largest scale) in the vertical from Table 2, we note that $\gamma_1^2<n(n+1)$ for

the scales of interest ($14 \leqslant n \leqslant 25$). We thus may approximate $E(\gamma_{n,1}) \approx n(n+1)|\psi_{n,1}|^2$ and from (9) and (10),

$$K = \frac{E}{1+\dfrac{\gamma_1^2}{n(n+1)}} \approx E \propto \{[n(n+1)]^{\frac{1}{2}}\}^{-3} \approx n^{-3},$$

$$A = \frac{\gamma_1^2}{n(n+1)} K \propto \{[n(n+1)]^{\frac{1}{2}}\}^{-5} \approx n^{-5}.$$

Thus, we see that although the kinetic energy will distribute with a -3 slope, the available potential energy will have a -5 slope. This result derived by Merilees and Warn for a two-level atmosphere is consistent with our result because the lowest vertical mode ($i=1$) from Table 2 would be the only mode available in such a vertically constrained model. Subsequent data analyses should assist in estimating the energy amplitude distribution in the vertical modes.

3. Data and representation

Since it was shown by Lorenz (1955) that temperature variance is a measure of available potential energy, the spectral distribution of potential energy will be described by a decomposition of temperature data in spherical harmonics, the appropriate eigenfunctions in a two-dimensional spherical surface. However, because of data paucity, no characteristic expansion was made in the vertical and only two-dimensional analyses in pressure surfaces will be presented. A similar analysis was made for the kinetic energy by the writer in KES[1] for the winter months of 1969. Comparable kinetic energy spectra in one dimension (planetary waves) may be found in the works of Wiin-Nielsen (1967) and Julian *et al.* (1970). Kao (1970) has produced limited one-dimensional temperature variance spectra, but no two-dimensional spectra appear to have been presented yet.

Five levels of temperature data (700, 500, 300, 250, 200 mb) available at 0000 and 1200 GMT for the months of January, February, March, 1970, have been utilized in the analysis. The data were taken at 2.5° latitude and longitude points from NMC analyses over all longitudes $0 \leqslant \lambda \leqslant 2\pi$ and latitudes $20 \leqslant \phi \leqslant 90$N. Corresponding data were taken from tropical analyses (Bedient) for the same 2.5° latitude and longitude points (where common) over all longitudes and $0 \leqslant \phi \leqslant 30$N latitudes. The data were then merged utilizing a linear weighting function for all longitudes between $20 \leqslant \phi \leqslant 30$N. Recent evaluation of merging procedures by Burrows (1974) tends to justify this merging region. Although the data used originated at NMC, convenience dictated utilizing NCAR as a data source. Unavailability of 1969 tropical temperature data at NCAR [the year for which kinetic energy spectra were analyzed (see KES)] led to our choice of 1970 as the analysis year.

The data were converted to spectral components, amplitude and phase of each scale element, by expansion in terms of *even* solid spherical harmonics to reflect the symmetry property of the temperature field with respect to the equator; Southern Hemispheric data are inadequate to provide a useful global analysis. Let the expansion be written as

$$T(\lambda_i,\mu_j,t,p) = \sum_\alpha T_\alpha(t,p) Y_\alpha(\lambda_i,\mu_j), \tag{11}$$

where t and p represent time and pressure, respectively, and α is the complex scaling index $\alpha \equiv n_\alpha + il_\alpha$; n_α is the two-dimensional spherical wavenumber, and l_α describes the planetary wavenumber on any latitude circle. Given data at the longitude and latitude points (λ_i,μ_j) specified above, and the orthogonal properties of the associated Legendre polynomials Y_α, Eq. (11) was inverted using the method suggested by Ellsaesser (1966) yielding values for the T_α at each time and pressure surface.[2] The maximum resolution allowed by the inversion for 2.5° data spacing is 36 waves, but we shall discard the shortest waves since they do not contain sufficient reality (see Julian *et al.*, 1970, or KES).

The available potential energy, presented as temperature variance, will be expressed through (11) as the autocorrelation of temperature coefficients T_α. If we define the potential energy as P,

$$P \approx c \int T^2 dA = c \sum_\alpha T_\alpha T_\alpha^* \equiv c \sum_\alpha P_\alpha. \tag{12}$$

We let c represent a scaling constant and the P_α represent the unscaled potential energy in each scale element α. By suitable summation of the elements P_α, we may discuss the available potential energy in either a one-dimensional or two-dimensional spectral distribution. For the one-dimensional representation in terms of planetary wavenumber l_α, let the energy in each l-scale be given by

$$P_l = \sum_{n_\alpha} P_\alpha, \tag{13}$$

where the summation proceeds over all n_α for given l. Correspondingly, the two-dimensional representation which depends only on n (see KES) will be given as

$$P_n = \sum_{l_\alpha} P_\alpha, \tag{14}$$

with the summation proceeding over all l_α for fixed n. The quantities P_α, P_n and P_l given at all pressure surfaces and times available were subsequently used to describe the spectral behavior of the available potential energy.

To see the statistical property of the energy in each scale element (α), we have taken the time mean of the

[1] KES will be the acronym used subsequently to describe the kinetic energy spectra presented by Baer (1972).

[2] More detail on this inversion procedure may be found in KES.

TABLE 3. Ratio of the potential energy spectral function calculated using the assumption of isotropy to the one using only data, at given pressure surfaces and for the wavenumbers $8 \leqslant l \leqslant 25$.

Pressure level	Wavenumbers																	
(mb)	8	9	10	11	12	13	14	15	16	17	18	19	20	21	22	23	24	25
700	1.14	1.07	0.98	1.27	1.22	1.29	1.31	1.37	1.24	1.18	1.22	1.12	1.27	1.44	1.36	1.53	1.27	1.68
500	1.03	0.94	1.00	1.14	1.14	1.10	1.15	1.25	1.10	1.05	1.12	1.24	1.29	1.36	1.54	1.52	1.38	1.75
300	1.00	0.83	0.69	0.84	0.73	0.86	0.79	1.02	0.91	0.83	0.94	0.92	1.17	1.15	1.21	1.30	1.49	1.86
250	0.96	0.89	0.80	0.96	0.90	0.94	0.88	1.00	0.93	0.94	1.09	1.16	1.11	1.36	1.33	1.43	1.37	1.76
200	0.71	0.80	0.74	0.88	0.71	0.75	0.69	0.86	0.55	0.62	0.72	0.83	0.80	0.93	0.92	0.93	1.00	0.99
Vertical mean	1.08	0.97	0.96	1.12	1.15	1.13	1.12	1.17	1.24	1.17	1.30	1.38	1.30	1.58	1.61	1.71	1.46	2.09

P_α and have also generated a vertical mean in pressure. This latter quantity was obtained by assuming the temperature coefficients to be expressed as a fourth-order polynomial in pressure (since only five data levels are available) and integrating and normalizing this polynomial over the layer 700–200 mb. The resulting averaged available potential energy per scale element (averaged in both time and pressure thus representing some mean atmospheric pressure surface) has been plotted on a diagram having l as the abscissa and $n-l$ as ordinate. The plotted diagram has been analyzed for isopleths of available potential energy and is presented in Fig. 1. Isopleths of the two-dimensional index (n) may be seen as the bold diagonal lines on the figure. It is interesting to note from Fig. 1 that in the region for $n \geqslant 15$, involving scales outside the primary baroclinic excitation range, the potential energy isopleths tend to parallel lines of constant two-dimensional index; a similar observation was found in the kinetic energy analyses (KES, Fig. 3). This result indicates that the spectral distribution of both kinetic and available potential energy in the mean winter atmosphere is effectively represented by the two-dimensional index n, and suggests that the isotropic assumption as suggested by Charney is valid. A more careful assessment of the isotropic assumption based on our data samples may be made by comparing the spectral function $P_1(l)$ when calculated with the coefficients $T_{n,l}$ with its value utilizing $P_2(n)$. For this purpose we show in Table 3 the ratio

$$R(l) \equiv \sum_{n=l}^{36} \frac{2-\delta_{l,0}}{2n+1} P_2(n) \Big/ \sum_{n=l}^{36} (2-\delta_{l,0}) |T_{n,l}|^2$$

with

$$P_2(n) = \sum_{l=0}^{n} (2-\delta_{l,0}) |T_{n,l}|^2,$$

for the pressure levels 200, 250, 300, 500 and 700 mb, the pressure mean, and for the range of scales $8 \leqslant l \leqslant 25$. It can be seen from the table that the isotropy condition is approached for many scales and at many levels since exact isotropy would give a value for $R=1$. Clearly the shorter scales ($l>18$) do not yield adequate data to satisfy the condition, whereas the longest scales ($8-12<l$) may still be in the energy generating range. Discussion of the vertical dependence awaits the three-dimensional data analysis. Finally, a rough estimate of c [Eq. (12)] indicates that equipartition between kinetic and potential energy also exists. This latter result must be considered with caution, however, since we are comparing data from two different years (but for the same season).

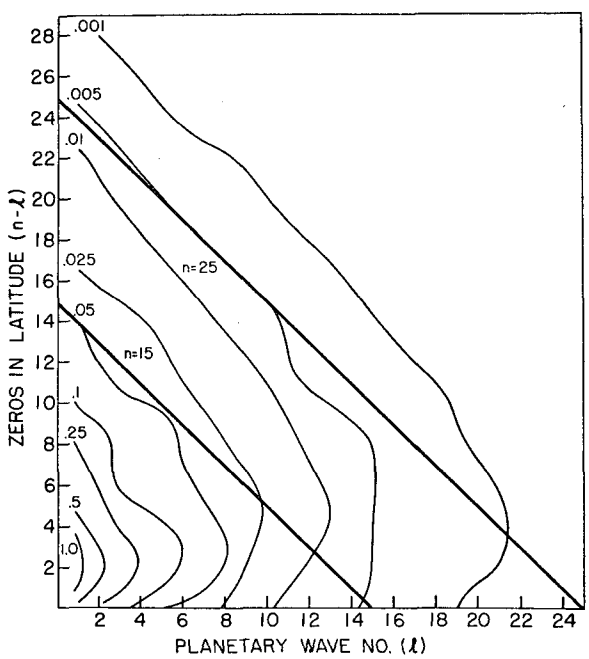

FIG. 1. Average temperature variance (both in height and time) in each two-dimensional wave component, $\alpha=n+il$, analyzed as a spectral map. Solid diagonal lines represent isopleths of constant two-dimensional index n.

4. Spectral properties

The potential energy distribution based on one- or two-dimensional spectra in isobaric surfaces may be represented by plotting the quantities P_l and P_n [Eqs. (13) and (14)] logarithmically against their cor-

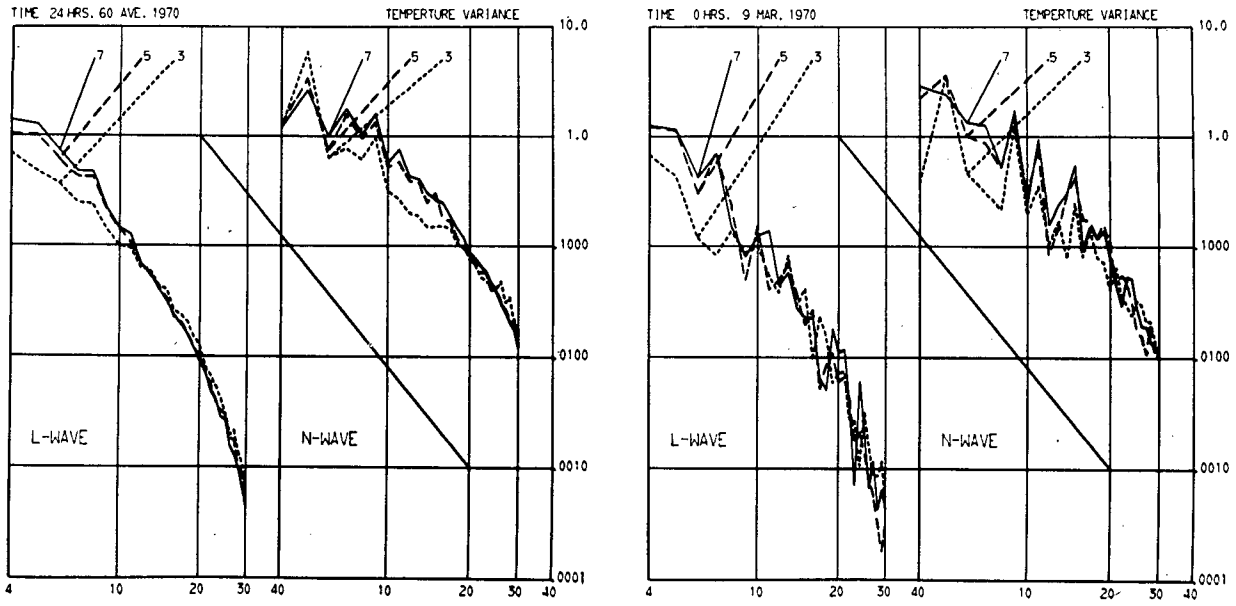

FIG. 2. Spectral distribution of temperature variance for the decibar levels 3, 5, 7. The left curves represent the planetary wave index (l) and right curves the two-dimensional index (n). The solid line has slope of -3. Time-averaged data are on the left plot, those for 0000 GMT 9 March 1970 on the right.

responding wavenumbers. Fig. 2 shows two such plots, with the distribution in one dimension (l-wave) on the left and that in two dimensions (n-wave) on the right. The solid line describes a -3 slope. Three different levels (7, 5 and 3 db) have been presented. The right hand plot represents data for 0000 GMT 9 March 1970, whereas the left plot is for data averaged over the entire sampling period. Clearly the daily variability is large, as is evident from comparison of these two plots, and any general properties of the spectral distribution can best be drawn from the averaged data.

Limits in data quality were established for kinetic energy (KES) and indicate that confidence may not be placed in data with excessively large scale numbers; $n>25$, $l>18$. Since this limit is based principally on observing station distribution rather than on the observed variable, we may apply similar limits to the temperature data. Thus, although we shall not draw conclusions from Fig. 2 in spectral regions which exceed the limits just prescribed, we have plotted the data for smaller scales to show what is available in the analyses from which the coefficients are derived. Since our concern in this study is with shorter scales we have excluded the largest scales (n, $l<4$) from the diagram.

We note from Fig. 2 that in the planetary wave representation, the temperature amplitude in the larger waves ($4\leqslant l\leqslant 10$) tends to decrease with height in the atmosphere, whereas it increases slightly for the shorter scales. The opposite behavior seems evident for the two-dimensional (n-wave) representation. There is, of course, some equivalence expected between the structure of the one-dimensional and two-dimensional spectra if isotropic conditions hold, but as we see from Fig. 1, the two-dimensional spectra incorporate more of the total scale variability in the data. Moreover, the larger energy amplitude in the two-dimensional representation for corresponding scale numbers—as much as an order of magnitude—is undoubtedly due to the number of scale elements (α) in each spectral component, P_n or P_l. Whereas the number of scale elements for each l-wave decreases with increasing l, the opposite is true for the n-wave. This may be seen from the limits on the sums in (13) and (14); the sum over l_α for given n goes as $0<l_\alpha\leqslant n$ ($l_\alpha\leqslant n$ is a condition inherent in the expansion) but the n sum proceeds as $l\leqslant n\leqslant n_{\max}$ where $n_{\max}=36$ for our expansion. A similar effect was evident in the kinetic energy analyses (KES).

There is some evidence of proximity to a -3 slope in the potential energy spectra (Fig. 2) in the region of acceptable data, a result also evident from the kinetic energy analyses. We may investigate the details of this distribution as follows. If we presume a logarithmic relationship between potential energy and scale number in the form

$$P_m=Am^b, \tag{15}$$

where m refers to either l (one-dimensional) or n (two-dimensional) wavenumber, we may fit the data described in Fig. 2 by least squares to (15) so long as we specify an initial and terminal index to define the scale range for which the slope (b) will be applicable. We have already noted that from analysis of kinetic energy, a suitable two-dimensional scale range is $14\leqslant n\leqslant 25$. It is this slope which may, if the conditions of geostrophic turbulence are satisfied in the observations, yield a value of -3. Fig. 3 shows some values of slope for both

one- and two-dimensional representations, for various initial and terminal index numbers, and for both the 300-mb surface and the vertical mean. The initial index values follow the curves whereas the terminal index values are noted on the abscissa. To compare the potential energy spectra with those of kinetic energy, several kinetic energy slope curves (dotted lines taken from Fig. 10 of KES) have been reproduced in Fig. 3.

We observe immediately that the slopes for the one-dimensional representation are significantly steeper than -3. They are given for index ranges which exceed data reliability and therefore express the effect of analysis rather than reality on spectral distribution. Since such data are used as initial conditions in numerical integrations, it is worthwhile to present them here. As one proceeds to terminal indices which approach data reliability, the magnitude of the slope decreases. Slope values extrapolated to yet smaller terminal index values compare favorably with the estimates given by Wiin-Nielsen (1967). For comparison with kinetic energy, we note that the curve for initial index 10 gives a steeper slope for potential energy than for kinetic energy in the vertical mean spectra. We may speculate that either the decay rate for temperature variance differs from kinetic energy in the spectral range $10 \leqslant l$ or that the analysis procedure for the temperature field differs from the wind analysis, with greater smoothing in the shorter scales.

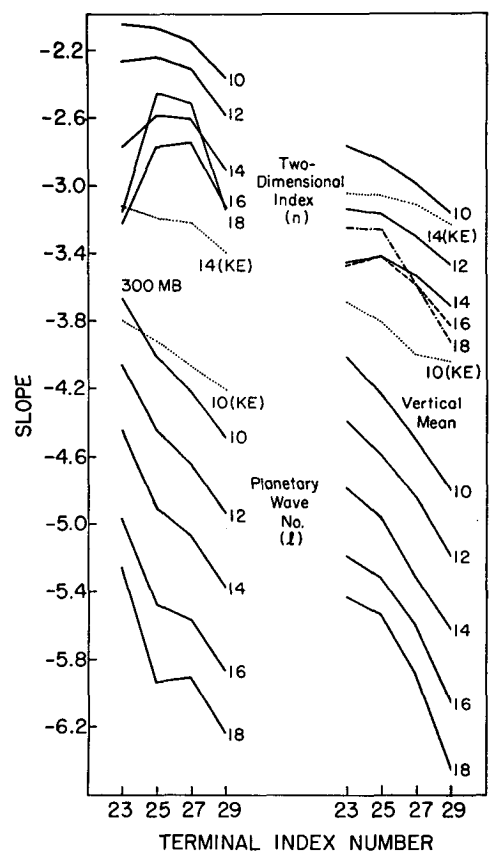

FIG. 3. Statistical slopes of time-averaged temperature variance (available potential energy) with scale [both one- and two-dimensional (l and n)] for different spectral regions. The abscissa denotes terminal index values and the number following curve denotes initial index. Kinetic energy statistics are included.

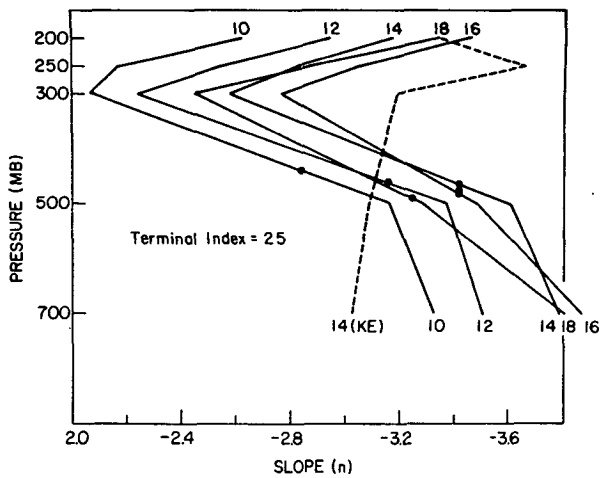

FIG. 4. Vertical variation of statistical slope (time averaged) of temperature variance for the two-dimensional scale index with terminal index value of 25 and initial index value on curves. Dots denote pressure mean slope and kinetic energy statistics are superimposed.

Let us now consider the potential energy spectra slopes in terms of the two-dimensional index (n). For scales outside the baroclinically active region ($n \gtrsim 14$), the slopes do not depend strongly on the terminal index, although as data reliability falls off ($n > 25$) the slope tends to steepen, an anticipated observation due to stronger smoothing of shorter scales in the analysis. There is a significant difference in the 300-mb slopes when compared to those of the vertical mean, a variability to be discussed subsequently. This variability is not so evident in the spectra of kinetic energy; note from the dotted curves for initial index 14 (taken from KES) on Fig. 3 that the corresponding temperature variance slopes are somewhat steeper in the vertical mean, and less steep at 300 mb.

Perhaps the most notable result expressed on Fig. 3 is the proximity to a -3 slope given for the two-dimensional spectra, and the much steeper slopes for the one-dimensional spectra. This latter effect may be due simply to lack of information in the shorter one-dimensional scales. Lack of isotropy between the one- and two-dimensional representations, however, as discussed earlier, may also play a role in this disparity and imply unacceptable amplitude in scales which do not satisfy the conditions for conservation of potential vorticity and the -3 slope. This feature of steeper slopes for one-dimensional analyses is also not unique to the available potential energy; similar observations were presented in our discussion of kinetic energy (see KES).

The variation of slope with decreasing pressure may be seen in Fig. 4, wherein we have plotted the slopes at the five available pressure surfaces for varying initial index values and a terminal index of $n=25$ (note that this diagram discusses the two-dimensional spectra variations only). The dot denotes the pressure mean slope, and we have superimposed the distribution of the kinetic energy slope in the range $14\leqslant n\leqslant 25$ for comparison. We observe a substantial decrease in magnitude of the slope up to 300 mb and then a sudden increase, in contrast to the kinetic energy slope which shows a pronounced maximum above 300 mb. This decrease, already noted in Fig. 3, was also observed in the one-dimensional analysis of Wiin-Nielsen (1967). The strong minimum in slope at 300 mb and its significant difference from -3 may reflect the pronounced variation in static stability and hence the Brunt-Väisälä frequency (N^2) at the tropopause level. Under these conditions, the geostrophic available potential energy, the quantity for which we anticipate a -3 spectrum, is not well represented by the temperature variance. Thus the test for -3 would best be made with the stream field rather than the temperature field. Even then, however, we might find substantial amplitude in vertical modes with characteristic scales significantly less than 14, thus leading to conditions unfavorable to a -3 distribution. At other levels where N^2 is not strongly variable, the temperature variance does give a good estimate of the available potential energy. The proximity of the spectra to -3 at any pressure surface then depends on the energy amplitude distribution in the vertical modes (see Section 2).

Referring to Fig. 4, we may conclude by observing that there appears to be relatively more available potential energy in the shorter scales as one proceeds vertically in the atmosphere to the tropopause whereas the opposite seems true for the kinetic energy. The physical interpretation of this effect is not immediately apparent.

5. Conclusions

Analyses of hemispheric kinetic energy data on constant pressure surfaces have shown, when decomposed into spectral form, a tendency toward a -3 slope with wavenumber, principally the two-dimensional wavenumber, in the appropriate scale range. Such a slope was anticipated from two-dimensional turbulence theory. However, since the atmosphere is three-dimensional in structure, two-dimensional theory is incomplete. Recent developments utilizing geostrophy suggest that the three-dimensional theory derived from the conservation of potential vorticity should yield a spectrum with a -3 slope in the appropriate three-dimensional scale range for both kinetic and available potential energy.

We have presented a possible three-dimensional spectral representation in terms of which the anticipated -3 slope may be verified from observation. Unfortunately, insufficient data are yet available for such an analysis. As an alternative we have analyzed the two-dimensional spectral form of temperature variance (a measure of available potential energy) in isobaric surfaces. If most energy resides in vertical modes which have similar scale indices to the horizontal modes in the spectral range where the -3 slope should exist, the two-dimensional analyses will be adequate in describing the three-dimensional spectra. The proximity of the calculated slopes of potential energy to -3 in our two-dimensional analyses gives an indication that in the scale range of applicability ($14\leqslant n\leqslant 25$ for the two-dimensional index) the energy resides in vertical modes which are in the appropriate range. That the energy amplitude is not in the largest vertical scales in the applicable range is suggested by the fact that no slopes near -5 exist, the expected slope for substantial amplitude in the largest vertical modes.

The data do not show consistent results on all pressure levels. More specifically, there is a pronounced change at the tropopause level. This result may well be due to the rapid change in stability there, causing a broadening of amplitude distribution in the vertical scales. Moreover, under these conditions the temperature variance is not an accurate representation of the geostrophic available potential energy for which the expected slope is valid. Nevertheless, the correspondence between the two-dimensional slope derived from both kinetic energy and available potential energy at most isobaric levels analyzed indicates promise in the statistical expectations of the geostrophic theory.

Further analyses of data in three-dimensional spectra are necessary. This may be accomplished by expansion of both temperature and wind data in vertical eigenfunctions such as Bessel functions or empirical orthogonal functions, provided such data are available on a hemispheric basis. With such expansions one may then isolate the appropriate three-dimensional scales for which the statistics (-3 slope) are predicted. Should the data corroborate the theory, one may then parameterize these scales in terms of their statistical expectation for inclusion as a closure scheme in numerical models. This procedure—to parameterize a portion of the scale region in terms of known or expected distributions—is in the final analysis essential for both the momentum and thermal fields if realistic long-range predictions are to be at all feasible.

Acknowledgments. The writer has benefited from discussions with Mr. Norman McFarlane. Data were kindly made available by Roy Jenne and Dennis Joseph from the files of the National Center for Atmospheric Research. Some computer time was provided by the Computer Facility of the National Center for Atmospheric Research. This research was supported by the National Science Foundation, Atmospheric Sciences Section, in part by Grant GA-11637 to Colorado State

University and in part by Grant GA-36409 to the University of Michigan.

REFERENCES

Baer, F., 1972: An alternate scale representation of atmospheric energy spectra. *J. Atmos. Sci.*, **29**, 649–664.

Burrows, W. R., 1974: Merging of data on NMC octagonal and Mercator grids for atmospheric analysis. *Mon. Wea. Rev.*, **102** (in press).

Charney, J. G., 1971: Geostrophic turbulence. *J. Atmos. Sci.*, **28**, 1087–1095.

Ellsaesser, H. W., 1966: Expansion of hemispheric meteorological data in antisymmetric surface spherical harmonic series. *J. Appl. Meteor.*, **5**, 263–276.

Gates, W. L., 1961: Static stability measure in the atmosphere. *J. Meteor.*, **18**, 526–533.

Julian, P. R., W. M. Washington, L. Hembree and C. Ridley, 1970: On the spectral distribution of large-scale atmospheric kinetic energy. *J. Atmos. Sci.*, **27**, 376–387.

Kao, S.-K, 1970: Wave number-frequency spectra of temperature in the free atmosphere. *J. Atmos. Sci.*, **27**, 1000–1007.

Kraichnan, R. H., 1967: Inertial ranges in two-dimensional turbulence. *Phys. Fluids*, **10**, 1417–1423.

Leith, C. E., 1971: Atmospheric predictability and two-dimensional turbulence. *J. Atmos. Sci.*, **28**, 145–161.

Lilly, D. K., 1969: Numerical simulation of two-dimensional turbulence. *Phys. Fluids*, Suppl. II, **12**, 204–249.

Lorenz, E. N., 1955: Available potential energy and the maintenance of the general circulation. *Tellus*, **7**, 157–167.

——, 1969: The predictability of a flow which possesses many scales of motion. *Tellus*, **21**, 289–307.

McFarlane, N. R., 1971: On the numerical evaluation of the structure of the various vertical modes in transient planetary waves. Tech. Rept. 002630-5-T, Dept. Atmos. Oceanic Sci., The University of Michigan, 33 pp.

Merilees, P. E., and T. Warn, 1972: The resolution implications of geostrophic turbulence. *J. Atmos. Sci.*, **29**, 990–991.

Simons, T. J., 1968: A three-dimensional spectral prediction model. Atmos. Sci. Paper No. 127, Colorado. State University, Fort Collins.

Wiin-Nielsen, A., 1967: On the annual variation and spectral distribution of atmospheric energy. *Tellus*, **19**, 540–559.

——, 1971: On the motion of various vertical modes of transient, very long waves. Part 1. *Tellus*, **23**, 87–98.